B Reference Material and Equations

In this appendix we gather a number of useful parameters and relationships for quick reference. We also give a brief description of the various magnetic indices used in ionospheric research, as well as definitions of some of the esoteric terms that creep into a discipline over the years.

B.1 Atmospheric and Ionospheric Structure

In this section we reproduce some tables and curves from the *Satellite Environment Handbook* (Johnson, 1961)[1] that offer a quick set of reference values for a number of ionospheric and atmospheric parameters, including such derived quantities as conductivity and collision frequency. The reader is cautioned that considerable information on the atmosphere has been accumulated since these curves were generated and that any detailed study should use newer sets of data. Nonetheless, these curves are internally consistent and have proved very useful over the years for quick estimates of the quantities displayed. For more specific conditions, see the MSIS model and other websites as given in Section B.4.

We start with four reference ionospheres, shown in Fig. B.1, that are representative of midlatitude conditions for daytime and nighttime and for two extreme portions of the solar cycle: solar maximum and solar minimum. To derive collision frequencies and conductivities from these plots an atmospheric model is necessary, due to the importance of the collisions with the neutral gas. The models used are given in Table B.1, which corresponds to solar maximum, and Table B.2, which corresponds to solar minimum.

[1] Material from Johnson (1961) is reproduced with the permission of Stanford Univ. Press. Copyright © 1961 by the Board of Trustees of the Leland Stanford Junior University.

The Earth's Ionosphere: Plasma Physics and Electrodynamics

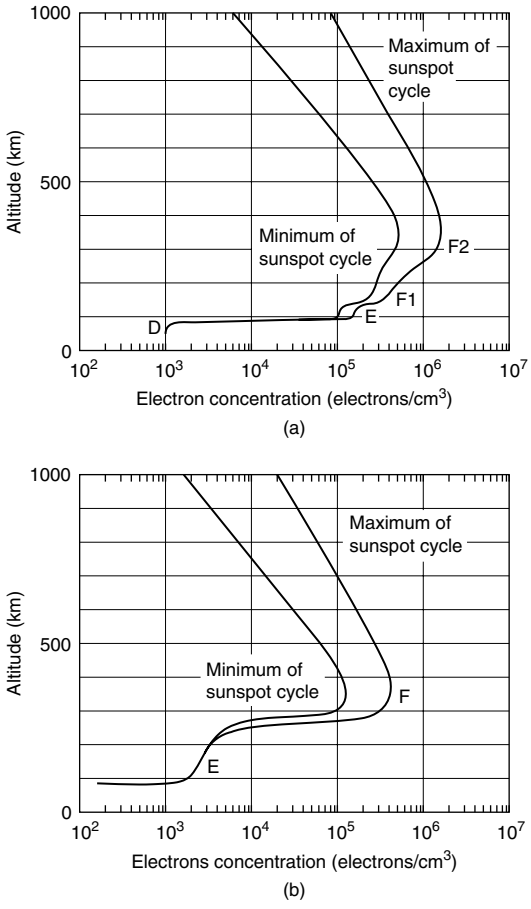

Figure B.1 Typical midlatitude distributions at the extremes of the sunspot cycle for daytime (a) and nighttime (b) conditions. [After Johnson (1961). Reproduced with permission of Stanford University Press. Copyright © 1961 by the Board of Trustees of the Leland Stanford Junior University.]

The first derived quantity is the ion collision frequency (Chapman, 1956), given by

$$\nu_{in} = \left(2.6 \times 10^{-9}\right)(n_n + n_i)\, A^{-1/2}\ \mathrm{s}^{-1}$$

where n_i is the ion concentration and n_n the neutral density in reciprocal cubic centimeters, and A is the mean molecular weight of the neutrals and ions, which are taken to be the same. The electrons are so light that they have little effect on the ions at ionospheric altitudes. The total collision frequency $\nu_i = \nu_{in} + \nu_{ie}$ then equals ν_{in}. In the magnetosphere, where n_n is essentially zero, ion-electron

Table B.1 Atmospheric Parameters as a Function of Altitude Near Sunspot Maximum[a]

h (km)	T (K)	M	n (particles/cm^2)	ρ (g/cm^3)	p (dyne/cm^2)	H (km)
0	288	29.0	2.5×10^{19}	1.22×10^{-3}	1.01×10^{6}	8.43
10	223	29.0	8.6×10^{18}	4.1×10^{-4}	2.65×10^{5}	6.56
20	217	29.0	1.85×10^{18}	8.9×10^{-5}	5.5×10^{4}	6.38
30	231	29.0	3.7×10^{17}	1.79×10^{-5}	1.19×10^{4}	6.83
40	261	29.0	8.3×10^{16}	4.0×10^{-6}	3.0×10^{3}	8.40
50	283	29.0	2.3×10^{16}	1.08×10^{-6}	9.0×10^{2}	8.11
60	245	29.0	7.53×10^{15}	3.7×10^{-7}	2.55×10^{2}	7.35
70	173	29.0	1.96×10^{15}	9.4×10^{-8}	4.7×10^{1}	5.21
80	168	29.0	2.84×10^{14}	1.36×10^{-8}	6.6×10^{0}	5.08
90	176	28.8	3.9×10^{13}	1.88×10^{-9}	9.5×10^{-1}	5.35
100	208	27.8	6.0×10^{12}	2.8×10^{-10}	1.74×10^{-1}	6.54
120	390	26.1	6.3×10^{11}	2.9×10^{-11}	3.4×10^{-2}	13.1
140	662	24.5	1.07×10^{11}	4.7×10^{-12}	1.04×10^{-2}	24.0
160	926	23.7	4.0×10^{10}	1.52×10^{-12}	5.1×10^{-3}	34.8
180	1115	22.8	2.0×10^{10}	7.7×10^{-13}	3.1×10^{-3}	43.6
200	1230	22.0	1.07×10^{10}	4.2×10^{-13}	1.95×10^{-3}	50.2
220	1305	21.2	6.6×10^{9}	2.7×10^{-13}	1.20×10^{-3}	55.3
240	1356	20.6	4.6×10^{9}	1.70×10^{-13}	8.5×10^{-4}	60.0
260	1400	20.0	3.3×10^{9}	1.12×10^{-13}	6.4×10^{-4}	63.8
280	1430	19.5	2.35×10^{9}	7.9×10^{-14}	4.7×10^{-6}	67.0
300	1455	19.1	1.82×10^{9}	5.7×10^{-14}	3.6×10^{-4}	70.6
320	1472	18.7	1.32×10^{9}	4.3×10^{-14}	2.7×10^{-4}	73.0
340	1485	18.4	1.00×10^{9}	3.1×10^{-14}	2.04×10^{-4}	75.6
360	1491	18.0	7.6×10^{8}	2.3×10^{-14}	1.54×10^{-4}	77.8
380	1496	17.8	5.9×10^{8}	1.78×10^{-14}	1.23×10^{-4}	79.9
400	1500	17.5	4.7×10^{8}	1.38×10^{-14}	9.8×10^{-5}	81.8
450	1500	17.0	2.5×10^{8}	7.2×10^{-15}	5.2×10^{-5}	85.7
500	1500	16.6	1.44×10^{8}	4.1×10^{-15}	2.9×10^{-5}	88.6
600	1500	16.3	4.8×10^{7}	1.32×10^{-15}	1.00×10^{-5}	93.1
700	1500	16.1	1.70×10^{7}	4.6×10^{-16}	3.5×10^{-6}	97.0
800	1500	16.0	6.3×10^{6}	1.66×10^{-16}	1.32×10^{-6}	101
900	1500	15.8	2.35×10^{6}	6.0×10^{-17}	4.9×10^{-7}	105
1000	1500	15.7	9.1×10^{5}	2.4×10^{-17}	1.90×10^{-7}	108
1200	1500	15.2	1.52×10^{5}	3.8×10^{-18}	3.2×10^{-8}	118
1400	1500	13.0	3.2×10^{4}	6.6×10^{-19}	6.7×10^{-9}	145
1600	1500	8.3	1.00×10^{4}	1.35×10^{-19}	2.1×10^{-9}	239
1800	1500	3.5	5.7×10^{3}	3.5×10^{-20}	1.14×10^{-9}	836
2000	1500	1.8	4.6×10^{3}	1.44×10^{-20}	9.5×10^{-10}	1167
2500	1500	1.0	3.47×10^{3}	6.0×10^{-21}	7.2×10^{-10}	2095

Source: Johnson (1961).

[a]The temperature T, molecular weight M, number concentration n, density ρ, and scale height H are given as functions of altitude h.

Table B.2 Atmospheric Parameters as a Function of Altitude Near Sunspot Minimum[a]

h (km)	T (K)	M	n (particles/cm^2)	ρ (g/cm^3)	p (dyne/cm^2)	H (km)
100	208	27.8	6.0×10^{12}	2.8×10^{-10}	1.74×10^{-1}	6.54
120	340	26.1	4.5×10^{11}	1.94×10^{-11}	2.1×10^{-2}	11.38
140	500	24.3	6.6×10^{10}	2.9×10^{-12}	4.6×10^{-3}	18.1
160	628	22.9	2.15×10^{10}	7.7×10^{-13}	1.86×10^{-3}	23.8
180	732	21.5	9.1×10^{9}	3.0×10^{-13}	9.1×10^{-4}	29.5
200	807	20.5	4.5×10^{9}	1.48×10^{-13}	5.0×10^{-4}	35.2
220	865	19.5	2.35×10^{9}	7.7×10^{-14}	2.8×10^{-4}	39.6
240	906	18.9	1.42×10^{9}	4.3×10^{-14}	1.77×10^{-4}	44.1
260	937	18.3	8.9×10^{8}	2.6×10^{-14}	1.14×10^{-4}	47.2
280	959	17.9	5.8×10^{8}	1.62×10^{-14}	7.6×10^{-5}	49.9
300	973	17.5	3.8×10^{8}	1.04×10^{-14}	5.1×10^{-5}	51.9
320	984	17.2	2.6×10^{8}	6.9×10^{-15}	3.5×10^{-5}	53.3
340	991	16.9	1.70×10^{8}	4.8×10^{-15}	2.34×10^{-5}	54.9
360	996	16.7	1.20×10^{8}	3.3×10^{-15}	1.66×10^{-5}	56.0
380	998	16.5	8.3×10^{7}	2.2×10^{-15}	1.14×10^{-5}	57.1
400	1000	16.3	6.0×10^{7}	1.58×10^{-15}	8.3×10^{-6}	58.4
450	1000	16.3	2.6×10^{7}	6.8×10^{-16}	3.6×10^{-6}	60.1
500	1000	15.9	1.20×10^{7}	3.1×10^{-16}	1.66×10^{-6}	61.6
600	1000	15.6	2.45×10^{6}	6.3×10^{-17}	3.4×10^{-7}	66.0
700	1000	14.7	5.8×10^{5}	1.28×10^{-17}	7.9×10^{-8}	76.0
800	1000	10.2	1.74×10^{5}	2.9×10^{-18}	2.4×10^{-8}	157
900	1000	5.1	9.1×10^{4}	7.21×10^{-19}	1.26×10^{-8}	312
1000	1000	2.3	7.1×10^{4}	2.7×10^{-19}	9.8×10^{-9}	487
1200	1000	1.3	5.3×10^{4}	1.07×10^{-19}	7.2×10^{-9}	915
1400	1000	1.0	4.5×10^{4}	7.6×10^{-20}	6.2×10^{-9}	1220
1600	1000	1.0	3.7×10^{4}	6.3×10^{-20}	5.1×10^{-9}	1319
1800	1000	1.0	3.1×10^{4}	5.6×10^{-20}	4.3×10^{-9}	1390
2000	1000	1.0	2.7×10^{4}	4.8×10^{-20}	3.8×10^{-9}	1456
2500	1000	1.0	2.0×10^{4}	3.4×10^{-20}	2.8×10^{-9}	1634

Source: Johnson (1961).

[a]The temperature T, molecular weight M, number concentration n, density ρ, and scale height H are given as functions of altitude h.

collisions must be considered. Curves of ν_i are given in Fig. B.2 for the two sunspot conditions. Since $n_i << n_n$, we need not distinguish between daytime and nighttime ionospheres.

The electron collision frequency ν_e depends on both neutral and ion terms. Nicolet (1953) has given the following expression:

$$\nu_{en} = \left(5.4 \times 10^{-10}\right) n_n T_e^{1/2} \text{ s}^{-1}$$

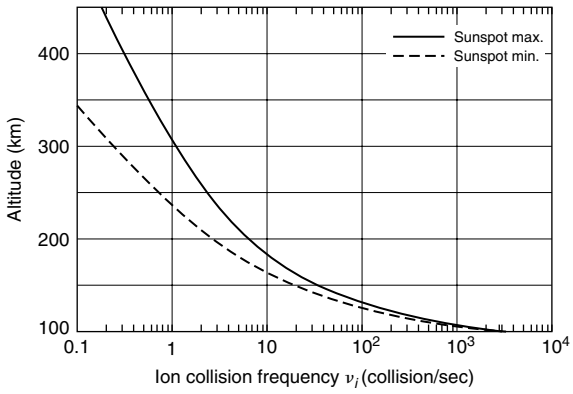

Figure B.2 Ion collision frequency versus altitude. [After Johnson (1961). Reproduced with permission of Stanford University Press. Copyright © 1961 by the Board of Trustees of the Leland Stanford Junior University.]

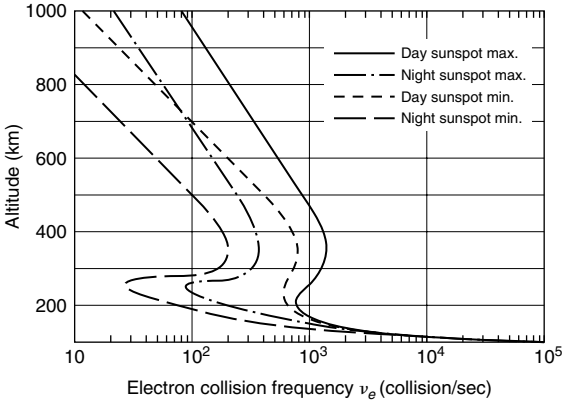

Figure B.3 Electron collision frequency versus altitude. [After Johnson (1961). Reproduced with permission of Stanford University Press. Copyright © 1961 by the Board of Trustees of the Leland Stanford Junior University.]

where n_n is again in reciprocal cubic centimeters and T_e is expressed in Kelvins. Similarly,

$$\nu_{ei} = (34 + 4.18 \ln)\left(T_e^3/n_e\right) n_e T_e^{-3/2} \text{ s}^{-1}$$

yields the Coulomb collision frequency. The sum of the two collision frequencies is presented in Fig. B.3 for the four possible combinations of conditions we are considering. In these plots $T_e \approx T_n$ at night and at low altitudes but is larger during the daytime due to heat transfer from photoelectron flux.

The parallel or specific conductivity σ_0 may now be calculated from the expression

$$\sigma_0 = ne^2(1/m\nu_e + 1/M\nu_i)$$

Notice that since ν_e is proportional to n, at high altitude σ_0 becomes independent of n and, in fact, is simply proportional to $T_e^{3/2}$. The results are presented in Fig. B.4.

The Pedersen conductivity is given by

$$\sigma_p = ne^2\left(\frac{\nu_e}{m(\nu_e^2 + \omega_e^2)} + \frac{\nu_i}{M(\nu_i^2 + \omega_i^2)}\right)$$

and is plotted in Fig. B.5. The magnetic field was taken to be 0.5gauss $= 5 \times 10^{-5}$ Tesla. The Hall conductivity is given by

$$\sigma_H = ne^2\left(\frac{\omega_e}{m(\nu_e^2 + \omega_e^2)} - \frac{\omega_i}{M(\nu_i^2 + \omega_i^2)}\right)$$

where ω_e and ω_i (the gyro frequencies) are positive numbers. This expression is equivalent to (2.39c), and is shown in Fig. B.6. Although not shown in Fig. B.6, the Hall conductivity usually cuts off sharply below 100 km altitude, since it is directly proportional to the electron density. This holds since the electrons $\mathbf{E} \times \mathbf{B}$ drift even as low as 80 km, since $\omega_e > \nu_e$, while the ions are locked into the neutral gas. In extremely energetic particle precipitation events, Hall currents can flow at altitudes considerably lower than 105 km.

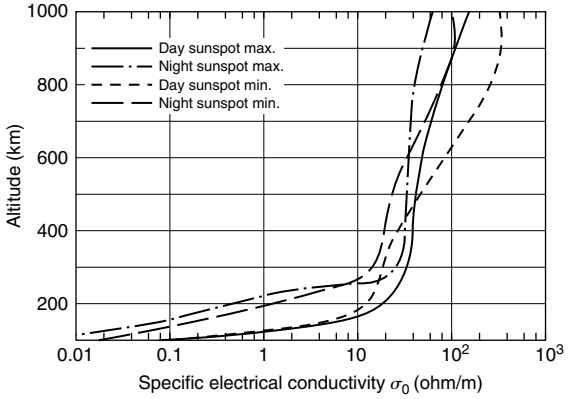

Figure B.4 Parallel electrical conductivity σ_0 (zero-field conductivity) versus altitude. [After Johnson (1961). Reproduced with permission of Stanford University Press. Copyright © 1961 by the Board of Trustees of the Leland Stanford Junior University.]

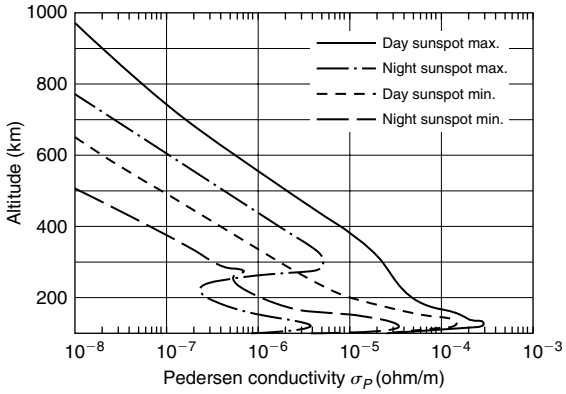

Figure B.5 Pedersen conductivity versus altitude. [After Johnson (1961). Reproduced with permission of Stanford University Press. Copyright © 1961 by the Board of Trustees of the Leland Stanford Junior University.]

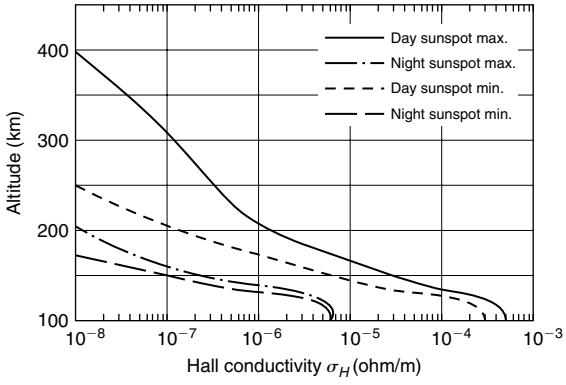

Figure B.6 Hall conductivity versus altitude. [After Johnson (1961). Reproduced with permission of Stanford University Press. Copyright © 1961 by the Board of Trustees of the Leland Stanford Junior University.]

The parameters ψ_0 and $1 + \psi_0$, which are used in E-region theory, are plotted for Jicamarca in Fig. B.7.

B.2 Miscellaneous Formulas

In these expressions B is in gauss (10^{-4} Tesla), n is in reciprocal cubic centimeters, $R_e = 6371\,\text{km}$ = one earth radius, temperature is expressed in electron volts, electric field is expressed in millivolts per meter, and A is in atomic mass units. Singly charged species are assumed. Many of the formulas were adapted from the "NRL Plasma Formulary" (Publication 0084-4040, Naval Research Laboratory, Washington, D.C., 20375-5000).

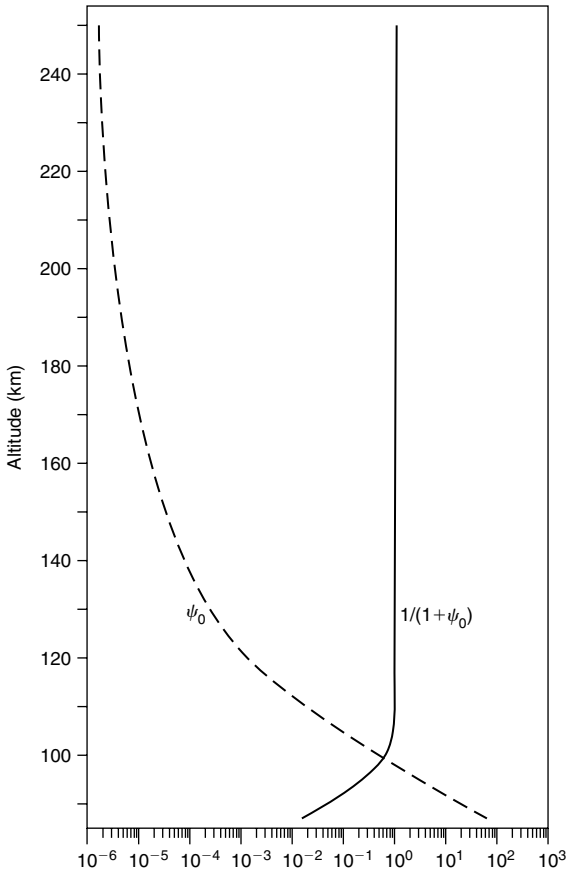

Figure B.7 Plots of ψ_0 and $1/(1+\psi_0)$ for equatorial parameters.

Earth's dipole magnetic field

$$|\mathbf{B}(r,\theta)| = \frac{0.3R_e^3}{r^3}\left(1+3\sin^2\theta\right)^{1/2}$$

$$\mathbf{B} = \frac{-0.6R_e^3\sin\theta}{r^3}\mathbf{a}_r + \frac{0.3R_e^3}{r^3}\cos\theta\mathbf{a}_\theta$$

where $\mathbf{a}_r$ is a unit vector radially outward, $\mathbf{a}_\theta$ is a unit vector in the direction of increasing θ, and θ is the magnetic latitude.

Equation for dipole field line

$$r = L\cos^2\theta$$

where L is the crossing point of the magnetic field at the magnetic equator measured in earth radii.

Magnitude of dipole field as a function of latitude on the same field line

$$B(\theta) = \left[B_e/\cos^6\theta\right]\left(1 + 3\sin^2\theta\right)^{1/2}$$

where B_e is the magnetic field value where the field line crosses the equator.

Electron plasma frequency

$$f_p = 8980\sqrt{n}\,\text{Hz}$$

Ion plasma frequency

$$f_{pi} = 210\sqrt{n/A}\,\text{Hz}$$

$$f_{pi}(\text{oxygen}) = 52.5\sqrt{n}\,\text{Hz}$$

Electron gyrofrequency

$$f_e = (\omega_e/2\pi) = 2.8 \times 10^6(B)\,\text{Hz}$$

Ion gyrofrequency

$$f_i = (\omega_i/2\pi) = 1.52 \times 10^3(B/A)\,\text{Hz}$$

$$f_i(\text{oxygen}) = 95(B)\,\text{Hz}$$

Lower hybrid frequency

(a) High-density limit $f_p > (\Omega_e/2\pi)$

$$f_{LH} = 6.52 \times 10^4\left(B/A^{1/2}\right)\,\text{Hz}$$

$$f_{LH}(\text{oxygen}) = 16.3 \times 10^4(B)\,\text{Hz}$$

(b) Low-density limit

f_{LH} = ion plasma frequency

Electron gyroradius

$$r_e = 2.38T_e^{1/2}/B\,\text{cm}$$

Ion gyroradius

$$r_i = 1.02A^{1/2}T_i^{1/2}/B\,\text{m}$$

Debye length

$$\lambda_d = 7.43 \times 10^2 T^{1/2}/n^{1/2}\,\text{cm}$$

Electron thermal velocity

$$V_{th}^e = \left(k_B T_e/m\right)^{1/2} = 4.19 \times 10^2 T^{1/2}\,\text{km/s}$$

Ion thermal velocity

$$V_{th}^i = \left(k_B T_i/M\right)^{1/2} = 9.79\,(T_i/A)^{1/2}\ \text{km/s}$$

Alfvén speed

$$V_A = 2.18 \times 10^6 B/\,(An)^{1/2}\ \text{km/s}$$

Beta

$\beta =$ thermal energy density/magnetic energy density

$$\beta = 4.03 \times 10^{-11} nT/B^2$$

Electron-ion collision frequency (va)

$$va \simeq w_p/N$$

B.3 Surface Magnetic Field Measurements and Magnetic Activity Indices

Equation (8.15) represents the fundamental relationships between horizontal and field-aligned currents and the electric field and conductivity in the ionosphere. The discussion of the dependence of the ionospheric conductivity on altitude given in Chapter 2 shows that the region over which substantial ionospheric currents flow perpendicular to the magnetic field lines is restricted to altitudes from about 90 to about 130 km in the sunlit ionosphere and may extend up to 300 km when no appreciable local ionization source is present. These horizontal currents are most easily detected from their magnetic field signature on the ground.

Ground-based magnetometers function somewhat differently from those on satellites, but their output—three mutually perpendicular components of the magnetic perturbation from a normal steady baseline—is the same. These magnetic field perturbations are usually resolved along the geographically north-south (positive north), east-west (positive east), and vertical (positive down) directions and are denoted by H, D, and Z components, respectively. Sometimes a geomagnetic coordinate system is used, in which case the symbols X, Y,

and Z denote the magnetic perturbations in the geomagnetic north, geomagnetic east, and parallel to **B** directions (in the Northern Hemisphere). It is impossible to derive the true horizontal ionospheric current distribution uniquely from ground magnetic perturbations, since they are a superposition of contributions from the horizontal ionospheric currents, field-aligned currents, distant currents in the magnetosphere, and currents induced in the earth's surface. For these reasons the ground magnetic perturbations are usually expressed in terms of "equivalent" ionospheric currents. The study of magnetic perturbations and their interpretation as current systems in the earth and in space is extremely complex and we do not discuss this topic in detail. However, magnetic perturbations are used to describe phenomena such as magnetic storms and substorms and to derive indices such as Dst, K_p, and AE that describe the magnetic activity in the earth's environment. It is therefore necessary to discuss briefly the nature of the measurements.

In the northern auroral zone this can be most simply done by considering the latitude profile of the magnetic perturbation produced by a current wedge of 3° latitudinal extent flowing westward through a 20° longitudinal extent of the ionosphere and closed by field-aligned currents at its edges. The resulting latitude profile for a meridian displaced 4° east of the center of the current wedge is shown schematically in Fig. B.8. Applying the right-hand rule for the magnetic perturbation, it can easily be seen that a maximum southward perturbation will exist directly under the current and it will diminish as we move to higher and lower latitudes. On either side of the current there will exist a vertical perturbation directed upward to the equatorward side and downward on the poleward side. Recall that the coordinate system we use is positive directed downward. The field-aligned currents will produce both north-south and east-west perturbations that have a nonzero effect because the current wedge has a finite longitudinal extent. The overhead horizontal current system will in general produce north-south and east-west perturbations, depending on the orientation of the current flow with respect to the magnetometer axes. In this case the contribution is purely in the north-south direction. It should be recognized that from any given magnetometer station the magnetic field perturbation is dependent on the strength of current system and its location with respect to the station.

The AE or auroral electrojet index is obtained from a number (usually greater than ten) of stations distributed in local time in the latitude region that is typical of the Northern Hemisphere auroral zone. For each of these stations, the north-south magnetic perturbation H is recorded as a function of universal time. A superposition of these data from all the stations enables a lower bound or maximum negative excursion of the H component to be determined; this is called the AL index. Similarly, an upper bound or maximum positive excursion in H is determined; this is called the AU index. The difference between these two indices, AU-AL, is called the AE index. Notice that negative H perturbations occur when stations are under an eastward-flowing current. Thus, the indices AU and AL give some measure of the individual strengths of eastward and

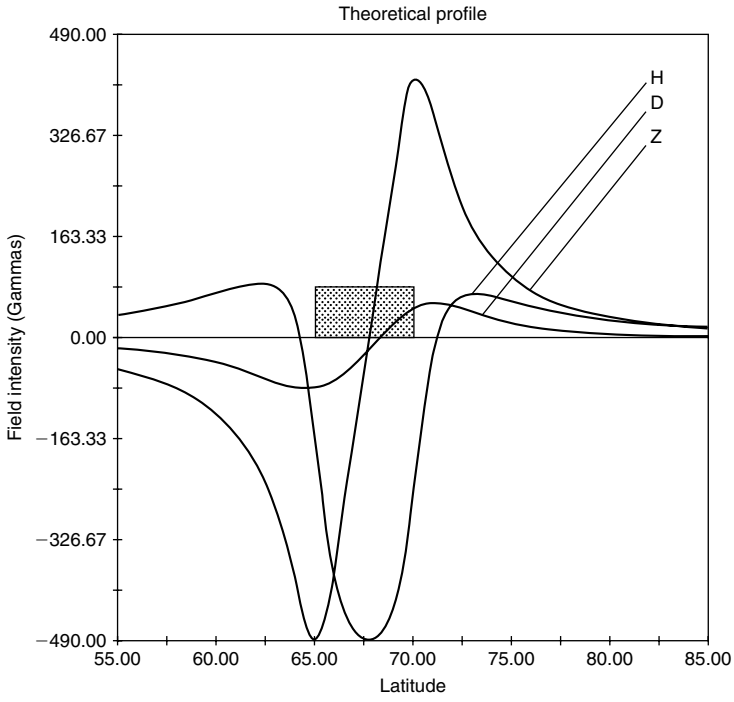

Figure B.8 Surface magnetic field perturbation for a current jet in the ionosphere. The curves show latitudinal profiles of H, D, and Z at a meridian displaced 4° east of the symmetry point. The conductivity of the earth and the associated image currents have been ignored. [After Kisabeth and Rostoker (1971). Reproduced with permission of the American Geophysical Union.]

westward electrojets, while AE provides a measure of the overall horizontal current strength. Significant excursions in the AE index from a nominal daily baseline are called magnetospheric substorms and may have durations of tens of minutes to several hours.

The K_p index is obtained from a number of magnetometer stations at midlatitudes. When these stations are not greatly influenced by the auroral electrojet currents, conditions are termed magnetically quiet. If the auroral zone expands equatorward; however, these stations can record the effects of the auroral electrojet current system and of the magnetospheric ring current and field-aligned currents that can connect it to the ionosphere. This occurs during so-called magnetically disturbed periods. The midlatitude stations are rarely directly under an intense horizontal current system and thus magnetic perturbations can be dominant in either the H or D component. The K_p index utilizes both these perturbations by taking the logarithm of the largest excursion in H or D over a 3-hour period and placing it on a scale from 0 to 9.

The Dst index is obtained from magnetometer stations near the equator but not so close that the E region equatorial electrojet dominates the magnetic perturbations seen on the ground. At such latitudes the H component of the magnetic perturbation is dominated by the intensity of the magnetospheric ring current. Recall that the ring current is directed westward at all local times and therefore produces a negative H perturbation at low-latitude magnetometer stations. The Dst index is a direct measure of the hourly average of this perturbation. Large negative perturbations are indicative of an increase in the intensity of the ring current and typically appear on time scales of about an hour. The decrease in intensity may take much longer, on the order of several hours. The entire period is called a magnetic storm with a relatively short main phase and a longer recovery phase. During a magnetic storm it is usual to observe several isolated or one prolonged substorm signature in the AE index.

The Dst index is calculated as an hourly index from the horizontal magnetic field component at four observatories, namely, Hermanus (33.3° north, 80.3° in magnetic dipole latitude and longitude), Kakioka (26.0° north, 206.0°), Honolulu (21.0° north, 266.4°), and San Juan (29.9° north, 3.2°). They are also relatively evenly spaced on longitude. The convolution of their magnetic variations forms the Dst index, measured in nT, which is thought to provide a reasonable global estimate of the variation of the horizontal field near the equator. The SYM-H index uses six of ten magnetometer stations to calculate the symmetric portion of the horizontal component magnetic field near the equator with a resolution of one minute. By using ten stations, data dropouts can be accounted for by replacing the lost data with a backup. Wanliss and Showalter (2006) compare these indices. Websites are provided.

The Dst and AE indices for a typical magnetic storm are shown in the lower two panels of Fig. B.9. Initially, Dst increases at about 2000 UT on March 31. This is called sudden commencement and is due to increased values of the current at the magnetopause, which shields the magnetosphere from the solar wind. In another viewpoint, the magnetosphere becomes compressed and the field strength increases at the surface of the earth. Polar magnetic activity then begins, as seen in the AE index. Ten or more magnetic substorms occur in the next 72 h. These substorms create auroras and drive horizontal current systems, which dissipate energy in the ionosphere at the rate shown by U_T in the second panel [units are (ergs/s) $\times 10^{-18}$].

As the substorms occur they energize plasma. Some of this precipitates into the atmosphere and some is driven deep into the inner magnetosphere. The latter causes the ring current, which makes a loop around the earth with a net positive current to the west. Such a current loop makes a magnetic perturbation in the southward direction at the earth that is roughly independent of longitude and that causes a net decrease in the earth's magnetic field. The Dst index therefore has a negative excursion which is the classical signature of a magnetic storm.

The top panel in Fig. B.9 is a measure of the energy flux in the solar wind times an area factor at the front of the magnetosphere (Akasofu, 1981). The

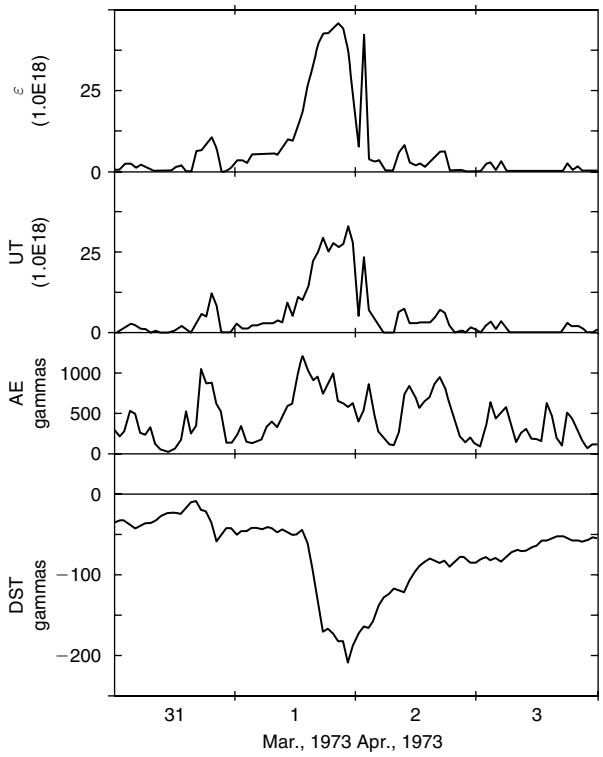

Figure B.9 Example of the relationship between the power where $\varepsilon = AV_{sw}B^2 \sin^4(\theta/2)$ equals the solar wind-magnetosphere energy flux and the total energy dissipation rate U_T (ergs/s) of the magnetosphere for the storm of March 31 to April 3, 1973. A is an effective area, B is the magnitude of the IMF, V_{sw} is the solar wind velocity, and θ is the clock angle of the IMF in the y-z plane, ($\theta = \tan^{-1}(B_y/B_z)$). The AE and Dst indices are also shown. (Figure courtesy of S.-I. Akasofu.)

agreement between the top two panels is quite remarkable and shows clearly that the system is solar wind driven.

References

Akasofu, S. I. (1981). Energy coupling between the solar wind and the magnetosphere. *Space Sci. Rev.* **28**, 121.

Chapman, S. (1956). The electric conductivity of the ionosphere: A review. *Nuovo Cimento* **5**, Suppl., 1385–1412.

Johnson, F. S., ed. (1961). *Satellite Environment Handbook*. Stanford Univ. Press, Stanford, California.

Kisabeth, J. L., and Rostoker, G. (1971). Development of the polar electrojet during polar-magnetic substorms. *J. Geophys. Res.* **76**, 6815–6828.

Nicolet, M. (1953). The collision frequency of electrons in the ionosphere. *J. Atmos. Terr. Phys.* **3**, 200.

Wanliss, J. A., and Showalter, K. M. (2006). High-resolution global storm index: Dst versus SYM-H. *J. Geophys. Res.* **111**, A02202, doi:10.1029/2005JA011034.